Effects of the plasma environment on the atomic structure and K-lines of He- and Li-like oxygen ions

J. Deprince[1], P. Palmeri[1], P. Quinet[1,2], S. Fritzsche[3,4], M. Bautista[5], C. Mendoza[5], T.R. Kallman[6], and J. Garcia[7]

[1]*Physique Atomique et Astrophysique, Université de Mons, B-7000 Mons, Belgium;* `Jerome.Deprince@umons.ac.be`, `Patrick.Palmeri@umons.ac.be`, `Pascal.Quinet@umons.ac.be`

[2]*IPNAS, Université de Liège, B-4000 Liège, Belgium*

[3]*Helmholtz Institut Jena, 07743 Jena, Germany*

[4] *Theoretisch Physikalisches Institut, Friedrich Schiller Universität Jena, 07743 Jena, Germany*

[5]*Department of Physics, Western Michigan University, Kalamazoo, MI 49008, USA*

[6]*NASA Goddard Space Flight Center, Code 662, Greenbelt, MD 20771, USA*

[7]*Department of Astronomy, California Institute of Technology, Pasadena, CA 91125, USA*

Abstract. The main goal of the present work is to estimate the effects of plasma environment on the atomic parameters associated with the K-vacancy states in oxygen ions of the helium and lithium isoelectronic sequences within the astrophysical context of accretion disks around black holes. In this purpose, multiconfiguration Dirac-Fock and AUTOSTRUCTURE computations have been carried out for these ions by considering a time averaged Debye-Hückel potential for both the electron-nucleus and electron-electron interactions in order to model the plasma environment. A new set of results obtained by these two methods concerning the plasma effects on ionization potentials, transition energies and radiative emission rates is reported for O VI and O VII.

1. Introduction

INPUT : ASTROPHYSICAL CONTEXT

...

The atomic data related to K-vacancy states in oxygen ions have already been worked out (Garcia *et al.* (2005)) and have been incorporated in the collisional-radiative code XSTAR developed at the NASA Goddard Space Flight Center (Kallman and Bautista (2001), Bautista and Kallman (2001)) in order to model the spectra and to evaluate the physical conditions in astrophysical photoionized plasmas. However, none of these atomic parameters takes into account the real astrophysical situation in which the ions are embedded in a plasma although, as recently mentioned by Smith and

Brickhouse (2014) in a review named *Atomic Data Needs for Understanding X-ray Astrophysical Plasmas*, the consideration of the effects due to the plasma environment is essential for the interpretation of astrophysical X-ray spectra observed by current X satellites. Moreover, in the case of accretion disks around black holes, it turns out that fitting the data over the model spectrum requires uncommonly high iron abundances (Garcia *et al.* (2015)), namely several times the solar value. Actually, recent magnetohydrodynamics (MHD) simulations of accreting black holes (of 10 $M_{\odot}$ and with an accretion rate of 10%) carried out by Schnittman *et al.* (2013) predict that the plasma physical conditions in the accretion disk should be characterized by a temperature ranging from 10^5 K to 10^7 K and an electron density ranging from 10^{18} cm^{-3} to 10^{21} cm^{-3}. Such a plasma environment, with a rather high electron density, can have significant effects on the atomic processes affecting line emissions and on the ionization balance of the ion species present in the plasma. In this work, we present a sample of results concerning the plasma environment effects on the structure and on the radiative parameters associated with K-vacancy states in He- and Li-like oxygen ions, namely O VI and O VII.

2. Theoretical methods

2.1. Atomic structure calculations

In this work, two independent theoretical methods have been used to model the atomic structures and to compute the radiative parameters for the above-mentioned ions, namely the purely relativistic multiconfiguration Dirac-Fock (MCDF) method, by using a combination of the GRASP92 (Parpia *et al.* (1996)) and of the RATIP (Fritzsche (2012)) codes, and the Breit-Pauli relativistic approximation as implemented in the AUTOSTRUCTURE code (Badnell (1997), Badnell (2011)).

In the MCDF approach, all the atomic state functions (ASFs), $\Psi(\gamma, P, J, M_J)$, are expanded in linear combinations of configuration state functions (CSFs) of the same parity and total angular momentum, $\Phi(\alpha_i, P, J, M_J)$, according to

$$\Psi(\gamma, P, J, M_J) = \sum_i c_i\, \Phi(\alpha_i, P, J, M_J)\,. \tag{1}$$

The CSFs are in turn taken as antisymetrized products of a common set of orthonormal monoelectronic spin-orbitals of the form

$$\varphi_{n\kappa m}(r,\theta,\phi) = \frac{1}{r}\begin{pmatrix} P_{n\kappa}(r)\,\chi_{\kappa m}(\theta,\phi) \\ iQ_{n\kappa}(r)\,\chi_{-\kappa m}(\theta,\phi)\end{pmatrix}, \tag{2}$$

where $P_{n\kappa}(r)$ and $Q_{n\kappa}(r)$ are, respectively, the large and the small component of the radial wavefunction, and the angular functions $\chi_{\kappa m}(\theta,\phi)$ are the spinor spherical harmonics. The α_i represent all the one-electron and intermediate quantum numbers needed to completely define the CSF, while γ is usually chosen as the α_i corresponding to the CSF with the largest weight $|c_i|^2$. The quantum number κ is given by $\kappa = \pm(j + 1/2)$ where j is the electron total angular momentum quantum number. The sign before the parenthesis in the κ definition is determined in such a way that it corresponds to the coupling relation between the electron orbital momentum, l, and its spin, s, *i.e.* $l = j \pm 1/2$. The radial functions $P_{n\kappa}(r)$ and $Q_{n\kappa}(r)$ are numerically represented on a logarithmic grid and are required to be orthonormal within each κ symmetry. In the MCDF variational procedure, the radial functions and the expansion coefficients c_i are optimized self-consistently.

In order to obtain the MCDF multiconfigurational expansions for O VI and O VII, the active space (AS) method was used. This latter consists in exciting the electrons from the reference configurations to a given active set of orbitals. For each of these ions, the AS was built by considering all the single and double excitations from the spectroscopic configurations to the $n = 2$ and $n = 3$ orbitals. More precisely, the reference configurations used to build the AS for O VI were $1s^22s$, $1s^22p$, $1s2p^2$ and 1s2s2p, while $1s^2$ and 1s2p were the reference configurations for the MCDF expansion of O VII. In the case of O VI, this gave rise to 515 CSFs, while the AS of O VII contains 98 CSFs. The computations were carried out with the extended average level (EAL) option, optimizing a weighted trace of the Hamiltonian using level weights proportional to $2J+1$. They were completed with the inclusion of the relativistic two-body Breit interaction and the quantum electrodynamic corrections (QED) due to self-energy and vacuum polarization. The MCDF wavefunctions generated by the GRASP92 code were then used in the RATIP program to compute the atomic structure and radiative parameters associated with the K-vacancy states in O VI and O VII.

INPUT : AUTOSTRUCTURE METHOD AND CALCULATIONS

...

2.2. Modeling of plasma screening effects

In both methods, the effects of the plasma screening on the atomic properties were modeled by considering a time-averaged Debye-Hückel (DH) potential for both the electron-nucleus and electron-electron interactions. In the MCDF/RATIP approach, this potential can be expressed, in atomic units (a.u.), by

$$V^{\mathrm{DH}}(r,\lambda) = -\sum_{i=1}^{N} \frac{Ze^{-\lambda r_i}}{r_i} + \sum_{j<i}^{N} \frac{e^{-\lambda r_{ij}}}{r_{ij}}\,, \qquad (3)$$

while in the AUTOSTRUCTURE method, the DH potential reads as

INPUT : ANALYTIC FORM OF THE DH POTENTIAL IN AUTOSTRUCTURE

(4)

where N is the number of bound electrons, r_i is the distance of the ith electron from the nucleus, and r_{ij} is the distance between the electrons i and j. The plasma screening parameter, λ, is the inverse of the Debye shielding length, λ_{De}, and can be expressed, in atomic units, in terms of the electron density, n_e, and of the temperature, T_e, of the plasma as

$$\lambda = \frac{1}{\lambda_{\mathrm{De}}} = \left(\frac{4\pi n_e}{kT_e}\right)^{1/2}. \qquad (5)$$

Thus, any given values of both the temperature and the electron density of the plasma correspond to a certain value of the screening parameter λ. In the astrophysical context of an accretion disk around black hole, the physical conditions predicted by the MHD simulations performed by Schnittman *et al.* (2013) which were discussed in the introduction correspond to screening parameter values up to about 0.1 a.u. (whereas the isolated ion case obviously corresponds to $\lambda = 0$ a.u.). For this reason, plasma environment effects were estimated for plasma conditions characterized by a screening parameter ranging from 0 a.u. to 0.1 a.u. The choice of the Debye-Hückel model potential for describing the effects of the plasma environment is motivated by the supposed physical conditions (see section 1) of a typical accretion disk. In such conditions, the environment can be characterized as a weakly coupled plasma since its corresponding coupling parameter Γ, which represents the ratio of the Coulomb potential interaction energy between two particles to the thermal energy, is markedly lower than unity ($0.0003 < \Gamma < 0.3$). An expression of the plasma coupling parameter is given in Piel (2010) as

$$\Gamma = \frac{e^2}{4\pi\varepsilon_0 d k T_e}\,, \tag{6}$$

for particles separated by a mean distance $d = (3/(4\pi n_e))^{1/3}$. In the case of weakly coupled plasmas ($\Gamma \ll 1$), it is well established that the plasma screening effects can be appropriately described using a Debye-Hückel model potential.

3. Results and discussion

The ionization potentials (IPs) and K-thresholds of O VI and O VII obtained with both the MCDF/RATIP and the AUTOSTRUCTURE methods using plasma screening parameter values of $\lambda = 0$ a.u. and $\lambda = 0.1$ a.u. are respectively reported in Table 1 and Table 2, whereas the radiative wavelengths and transition probabilities (A) of the strongest K-lines ($A \geq 10^{11}$ s^{-1}) in those two ions computed by the same approach are respectively given in Table 3 and Table 4.

Table 1. Variation of the ionization potential (IP, in eV) of O VI and O VII computed by MCDF/RATIP and AUTOSTRUCTURE with the plasma screening parameter λ (in a.u.). The NIST values (Edlén (1979), Drake (1988)) are also given. $\Delta\text{IP} = \text{IP}(\lambda = 0.1) - \text{IP}(\lambda = 0.0)$.

		MCDF/RATIP			AUTOSTRUCTURE		
Ion	NIST	$\lambda = 0.0$	$\lambda = 0.1$	ΔIP	$\lambda = 0.0$	$\lambda = 0.1$	ΔIP
O VI	138.1189(21)[a]	135.71	120.06	-15.65	137.75	122.13	-15.62
O VII	739.32679(6)[b]	737.47	718.59	-18.88	738.89	720.12	-18.77

[a] Semi-empirical calculations in Li-like ions Edlén (1979)
[b] Theoretical energy calculations in He-like ions Drake (1988)

As one can note, for the isolated ion case ($\lambda = 0$ a.u.), the results obtained by MCDF/RATIP and AUTOSTRUCTURE are in very good agreement for the IPs and K-thresholds (within 1%) as well as for the radiative parameters (within 0.2% for the wavelengths and about 10% for the A-values) except for two transitions in O VI (1s2s2p $^2P_{1/2,3/2}$ - 1s^{2}2s $^2S_{1/2}$) for which a larger disagreement is observed for the transition probabilities. This may be explained by the strong mixing in the composition of the corresponding eigenstates obtained with the MCDF approach, which makes them very sensitive to configuration interaction. Moreover, a very good agreement is also found with the computations made by Garcia *et al.* (2005) using the pseudo-relativistic Hartree-Fock (Cowan (1981)) method for the K-line wavelengths (within less than 0.1%) and

Table 2. Variation of the K-threshold (in eV) of O VI and O VII computed by MCDF/RATIP and AUTOSTRUCTURE with the plasma screening parameter λ (in a.u.). ΔK-threshold = K-threshold(λ = 0.1) − K-threshold(λ = 0.0).

	MCDF/RATIP			AUTOSTRUCTURE		
Ion	$\lambda = 0.0$	$\lambda = 0.1$	ΔK-threshold	$\lambda = 0.0$	$\lambda = 0.1$	ΔK-threshold
O VI	695.31	679.10	-16.21	697.16	681.01	-16.15
O VII	737.47	718.59	-18.88	738.89	720.12	-18.77

A-values (10%), except again for the two problematic transitions mentioned above for which only our AUTOSTRUCTURE results agree with those from Garcia *et al.* (2005), whereas the MCDF/RATIP results differ by a factor 2 or 3. As a result, MCDF/RATIP data for these two transitions are to be taken very carefully as they should not be very reliable. It is also worth mentioning that the IPs computed by AUTOSTRUCTURE are closer to the NIST values than those calculated with the MCDF/RATIP method, whereas it is the opposite situation regarding the radiative parameters when comparing our data to experiments for most transitions, *i.e.* the MCDF/RATIP results are in general (except for the two transitions with dubious MCDF/RATIP results) in better agreement with experimental data than the AUTOSTRUCTURE ones. This is explained by the different models and strategies used to optimize the orbitals in the two approaches : in the AUTOSTRUCTURE computation, only the $n = 2$ correlation orbitals are included, while the MCDF model include configurations arising from all the single and double excitations to $n = 2$ and $n = 3$ orbitals that are optimized using the EAL option (see section 2.1) in order to better describe the high-lying K-vacancy states.

Table 3. Plasma effects on the K-line radiative wavelengths (in Å) in O VI and O VII computed by MCDF/RATIP and AUTOSTRUCTURE.

		MCDF/RATIP		AUTOSTRUCTURE	
Transition	Exp.	$\lambda = 0.0$	$\lambda = 0.1$	$\lambda = 0.0$	$\lambda = 0.1$
O VI					
$1s(^2S)2s2p(^3P)\ ^2P_{1/2}$ - $1s^22s\ ^2S_{1/2}$	22.0194[a]	22.0469	22.0634	22.0743	22.0893
$1s(^2S)2s2p(^3P)\ ^2P_{3/2}$ - $1s^22s\ ^2S_{1/2}$	22.0194[a]	22.0459	22.0624	22.0723	22.0873
$1s(^2S)2s2p(^1P)\ ^2P_{1/2}$ - $1s^22s\ ^2S_{1/2}$	21.82[b]	21.8860	21.9035	21.8496	21.8640
$1s(^2S)2s2p(^1P)\ ^2P_{3/2}$ - $1s^22s\ ^2S_{1/2}$	21.82[b]	21.8843	21.9018	21.8498	21.8642
O VII					
$1s2p\ ^1P_1$ - $1s^2\ ^1S_0$	21.6020[c]	21.6110	21.6291	21.6595	21.6766

[a] Electron beam ion trap measurements (Schmidt *et al.* (2004))
[b] Spectroscopic tables (Moore (1998))
[c] Spectroscopic measurements (Engström and Litzén (1995))

Regarding the plasma environment effects on the IPs and K-thresholds (the effect is very similar on these 2 parameters) with respect to the isolated ion case, one can note by looking at Table 1 and Table 2 that the results obtained by the MCDF/RATIP and the

Table 4. Plasma effects on the K-line radiative transition probabilities (in s^{-1}) in O VI and O VII computed by MCDF/RATIP and AUTOSTRUCTURE.

Transition	MCDF/RATIP		AUTOSTRUCTURE	
	λ = 0.0	λ = 0.1	λ = 0.0	λ = 0.1
O VI				
$1s(^2S)2s2p(^3P)\ ^2P_{1/2}$ - $1s^22s\ ^2S_{1/2}$	3.308E+12	3.293E+12	2.916E+12	2.900E+12
$1s(^2S)2s2p(^3P)\ ^2P_{3/2}$ - $1s^22s\ ^2S_{1/2}$	3.331E+12	3.316E+12	2.942E+12	2.926E+12
$1s(^2S)2s2p(^1P)\ ^2P_{1/2}$ - $1s^22s\ ^2S_{1/2}$	1.541E+11	1.490E+11	3.615E+11	3.611E+11
$1s(^2S)2s2p(^1P)\ ^2P_{3/2}$ - $1s^22s\ ^2S_{1/2}$	1.307E+11	1.260E+11	3.356E+11	3.355E+11
O VII				
$1s2p\ ^1P_1$ - $1s^2\ ^1S_0$	3.763E+12	3.743E+12	3.594E+12	3.576E+12

AUTOSTRUCTURE methods are in excellent agreement concerning the shifts. They both predict that, in the most "extreme" plasma conditions considered in our study (*i.e.* λ = 0.1 a.u., see section 1), the ionization potentials and K-thresholds of O VI and O VII are respectively lowered by about 16 eV and 18 eV in comparison with those corresponding to the isolated ions. Moreover, as shown in Figure 1, the lowering of the IPs is linear with the plasma screening parameter λ, and exactly the same behavior is observed for the K-thresholds. Such a lowering several eV of the IPs and K-thresholds may involve some modifications in the description and the composition of the medium, especially by affecting the ionization balance and the K-shell photoionization cross-sections, and therefore the astrophysical spectrum.

However, the radiative wavelengths and transition probabilities related to K-lines are only very weakly affected by plasma environment effects, as it can be seen by looking at Table 3 and Table 4. Actually, all the K-lines are redshifted by about 0.01-0.02 **Å**, while the A-values are all reduced by less than 0.5% in comparison with the isolated ion case (except for the MCDF/RATIP values corresponding to the two transitions discussed above which should not be reliable). One can also note by looking at Figure 2 and Figure 3 that, unlike the IP and K-threshold cases, the variation observed for the K-line radiative wavelengths and transition rates with the plasma screening parameter is not linear. Nevertheless, in contrast with the IP and K-threshold lowering, such small variations in the radiative parameters seem to be too weak to have a significant impact in the spectrum. Finally, let's also highlight that, here again, for the radiative parameters, the variations due to plasma effects relatively to the isolated ion case computed by the MCDF/RATIP and by the AUTOSTRUCTURE methods are in very good agreement.

A similar study of plasma environment effects on atomic structures and radiative parameters related to K-lines have already been carried out by Deprince *et al.* (2017) for the iron ions of the same isoelectronic sequences as O VI and O VII (helium and lithium), namely Fe XXIV and Fe XXV. In that work, it was found that, in plasma conditions such that λ = 0.1 a.u., the IPs and K-thresholds of Fe XXIV and Fe XXV were respectively lowered by about 65 eV and 68 eV with respect to the isolated ion case, which is a larger effect compared to the corresponding He- and Li-like oxygen ions. They also predict that, in such plasma conditions, all the K-lines in these two iron ions were redshifted, but the shifts are even weaker than those calculated for O VI and

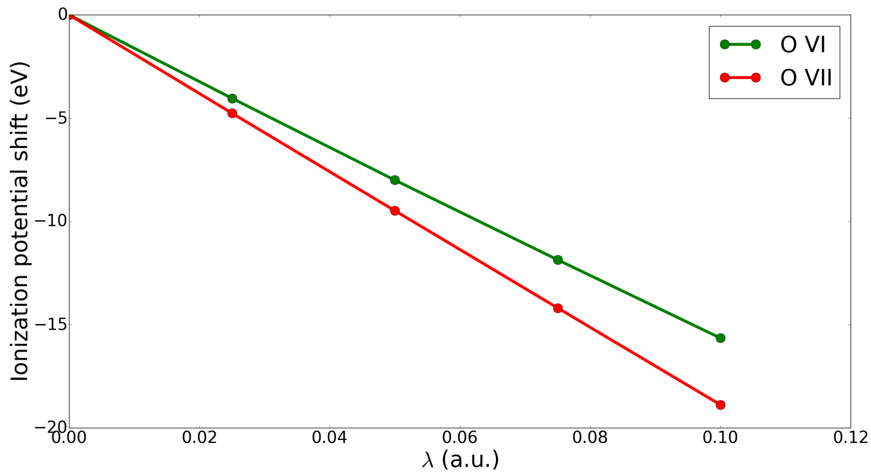

Figure 1. Plasma effects on the ionization potential (IP) of O VI and O VII computed by MCDF/RATIP.

O VII (about 10^{-4} Å). However, variations in transition probabilities were of the same magnitude except that some of them increase while others decrease.

4. Conclusion

To do

Acknowledgments. J.D. is Research Fellow of the Belgian Fund for Research Training in Industry and Agriculture (FRIA) while P.P. and P.Q. are, respectively, Research Associate and Research Director of the Belgian Fund for Scientific Research (F.R.S.-FNRS). Financial supports from these organizations, as well as from the NASA Astrophysics Research and Analysis Program (proposal number APRA15-0114) are gratefully acknowledged.

References

Badnell N.R., J. Phys. B : At. Mol. Opt. Phys. **30**, 1 (1997)
Badnell N.R., Comput. Phys. Commun. **182**, 1528 (2011)
Bautista M.A. and Kallman T.R., Astrophys. J. Suppl. Ser. **134**, 139 (2001)
Cowan R.D., *The Theory of Atomic Structures and Spectra*, University of California Press, Berkley (1981)
Deprince J., Fritzsche S., Kallman T.R., Palmeri P. and Quinet P., Am. Inst. of Phys. Conf. Proc. **1811**, 040002 (2017)
Drake G.W.F., Can. J. Phys. **66**, 586 (1988)
Edlén B., Phys. Scr. **19**, 255 (1979)
Engström L. and Litzén U., J. Phys. B. **28**, 2565 (1995)
Fritzsche S., Comput. Phys. Commun. **183**, 1523 (2012)
Garcia J., Mendoza C., Bautista M.A., Gorczyca T.W., Kallman T.R. and Palmeri P., Astrophys. J. Suppl. Ser. **158**, 68 (2005)

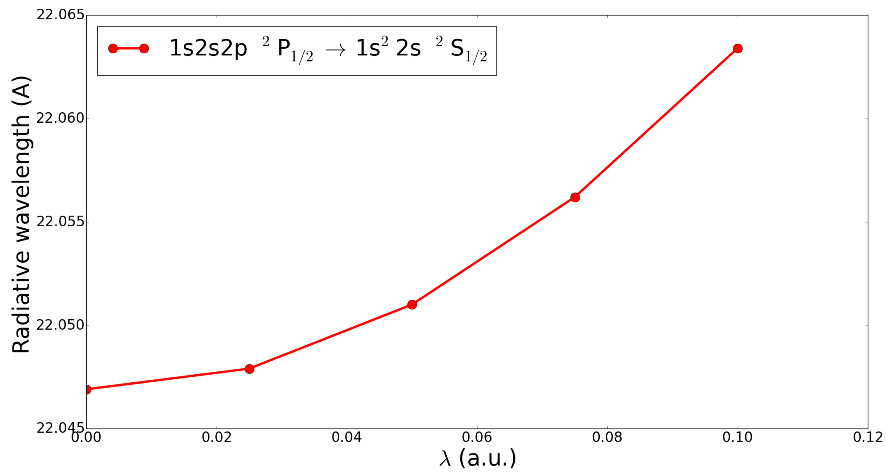

Figure 2. Plasma effects on a K-line radiative wavelegth of O VI computed by MCDF/RATIP.

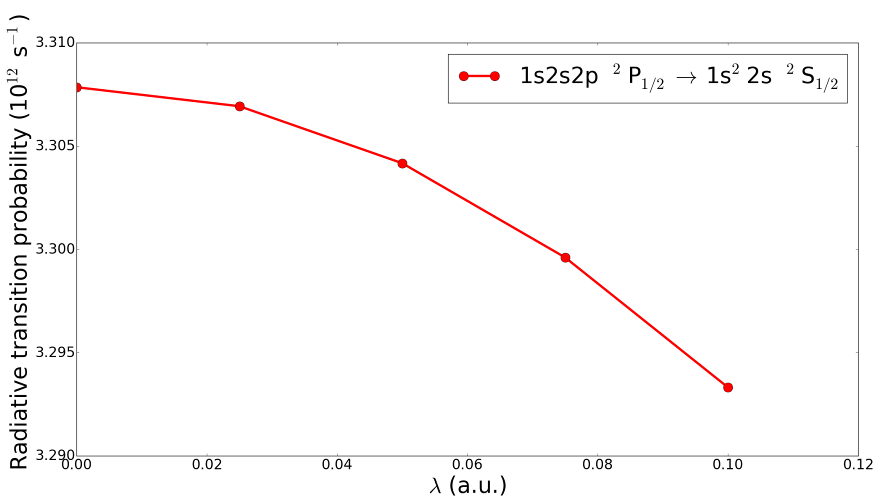

Figure 3. Plasma effects on a K-line radiative transition probability of O VI computed by MCDF/RATIP.

Garcia J., Steiner J., McClintock J., Remillard R., Grinberg V. and Dauser T., Astrophys. J. **813**, 84 (2015)
Kallman T.R. and Bautista M.A., Astrophys. J. Suppl. Ser. **133**, 221 (2001)
Moore C. E., *Tables of Spectra of Hydrogen, Carbon, Nitrogen and Oxygen Atoms and Ions*, ed. J.W. Gallagher (1998)
Parpia F.A., Froese Fischer C. and Grant I.P., Comput. Phys. Commun. **94**, 249 (1996)
Piel A., *Plasma Physics. An Introduction to Laboratory, Space and Fusion Plasmas*, Springer-Verlag (2010)
Schmidt M., Beiersdorfer P., Chen H., Thorn D.B., Träbert E. and Behar E., Astrophys. J. **604**, 562 (2004)
Schnittman J.D. Krolik J.H. and Noble S.C., Astrophys. J. **769**, 156 (2013)
Smith R.K. and Brickhouse N.S., Adv. At. Mol. Opt. Phys. **63**, 271 (2014)